

30 credit Master's thesis
November 2018

Excited States in Variational Many-Body Approaches

David Gustavsson
Supervisor: Gillis Carlsson



LUNDS UNIVERSITET
Lunds Tekniska Högskola

Abstract

A method is implemented wherein numerical approximations to the ground and first few excited states of a quantum mechanical N -body 1D harmonic oscillator are found through variational methods, representing the states as a linear combination of normalized pseudo-states which are themselves linear combinations of non-orthogonal Slater determinants. These states are then used as a low energy basis for configuration interaction. An expression is derived for an analytical matrix derivative of the energy functional, in order to improve the speed of the variation.

The speed and accuracy using the analytical derivative is compared to that of the numerical derivative, and a number of different gradient descent methods are tried and compared.

Acknowledgements

In writing this thesis, I have had great help from a number of people, and I would like to thank them: My supervisor Gillis Carlsson, who enthusiastically offered several ideas for projects and angles as soon as I asked, and who has continuously supplied feedback, insight and perspective. Claes Rogius Svensson, who wrote the thesis and code on which mine are built, and who provided me with a shortcut to understanding the project. The other thesis workers in room C367A. The Division of mathematical physics. My girlfriend who graciously tried to understand what I was talking about, and my family who graciously did not ask.

Notation

Notation	Definition	Description
$\delta_{i,j}$	$= \begin{cases} 1 & i = j \\ 0 & i \neq j \end{cases}$	Kronecker delta
$\delta_{(x-y)}$	$\int_{X \ni y} dx \delta_{(x-y)} f(x) = f(y)$	Dirac delta
$\lfloor x \rfloor$	$= \max\{m \in \mathbb{Z} m \leq x\}$	Floor function
\mathbf{X}_A	$= \mathbf{X}_{q_A}^{e_A}$	Merged index
\mathbf{X}_\star	$= \mathbf{X}_Q^E$	Last entry, subject to variation
\mathbf{X}_\bullet	$= (X_1 \ X_2 \ \cdots \ X_I)$	Slice
$\mathbf{X}_{<I}$	$= (X_1 \ X_2 \ \cdots \ X_{I-1})$	Partial slice
\sum_q	$\Leftrightarrow \sum_{q=1}^Q$	Sum over all determinants
\sum_e	$\Leftrightarrow \sum_{e=0}^E$	Sum over all pseudo-states
$\mathbb{0}, \mathbb{1}$		Zero-matrix, identity-matrix
$\mathbf{J}_{(i)}$	$(\mathbf{J}_{(i)})_k = \delta_{i,k}$	Single element vector
$\mathbf{J}_{(i,j)}$	$(\mathbf{J}_{(i,j)})_{kl} = \delta_{i,k} \delta_{j,l}$	Single element matrix
$\{\hat{A}, \hat{B}\}$	$= \hat{A}\hat{B} + \hat{B}\hat{A}$	Anti-commutator

Contents

1	Introduction	6
2	Theory	6
2.1	Model	7
2.1.1	Potential landscape	7
2.1.2	States	8
2.1.3	Properties of the Slater determinants	9
2.2	Gradient descent	10
2.2.1	Proportional descent	11
2.2.2	Rprop	11
2.2.3	Stiefel descent	12
2.3	Gradients	12
2.4	Configuration Interaction	13
3	Results	14
3.1	Gradients	14
3.2	Descent methods	14
3.3	Accuracy	14
3.4	Number of particles	17
3.5	Time complexity	17
3.6	Configuration interaction	17
3.7	Physical interpretation of results	21
4	Discussion	24
4.1	Conclusion	24
4.2	Extensions	24
	Appendix A Coefficients	27
A.1	Method for intra-state coefficients	27
A.2	Method for inter-state coefficients	27
	Appendix B Analytic derivatives of the energy functional	29

1 Introduction

The quantum mechanical N body problem, describing the wave functions of N interacting particles, is a famously complex and important problem in quantum mechanics. It is important for many fields in physics, including nuclear, atomic and solid state physics. Even worse than its classical counterpart, the quantum mechanical N body problem cannot be solved analytically in general for $N \leq 2$, which means that all larger systems need to be approximated and solved numerically. Efficient approximations are in high demand, and many different methods have been proposed.

One important method is known as *Hartree-Fock*, where the best 1-Slater determinant description is found by minimizing the energy, which gives a decent approximation for low interaction strengths. This method can be improved in several different ways, known as *post-Hartree-Fock* methods. One such method is *Configuration Interaction*, where a basis is formed by the Hartree-Fock solution together with a set of its excitations and the resulting Hamiltonian matrix is diagonalized. Full CI, where all Slater determinants are used as a basis, solves the N body problem exactly, but requires diagonalization of a very large matrix, so larger systems become time intensive. Truncating the basis can improve the speed considerably, but needs to be done intelligently – which determinants can be left out without sacrificing too much accuracy?

In this thesis a method is implemented to find Slater determinants associated with low energies, forming a manageably sized basis which can accurately describe the ground and first few excited states of an N -body system. The starting point for the investigation is the *Variation After Mean field Projection In Realistic model spaces* (VAMPIR), and its developments *Fed*, *Excited* and *Fed Excited VAMPIR* discussed in [6]. These methods were described over 30 years ago, but are becoming increasingly feasible using modern computer clusters, largely due to the fact that they can be parallelized. They entail finding the Hartree-Fock-solution through gradient descent, and then increasing the accuracy (Fed VAMPIR), the excitation level (Excited VAMPIR) or both (Fed Excited VAMPIR) by adding more Slater determinants.

2 Theory

In this section, the problem to be solved is introduced in greater detail, as well as the structure of the solution and the methods of gradient descent and differentiation to be compared.

2.1 Model

2.1.1 Potential landscape

This thesis treats N interacting fermions in a 1D quantum harmonic oscillator (HO) potential, $V(x) = (\omega x)^2$. The harmonic oscillator closely mimics, among other things, the coulomb potential felt by electrons in presence of a positively charged nucleus, and the extension to 3D for atomic physics is almost trivial.

For atomic and nuclear physics, most important particles are fermionic, which is why they are treated here. A similar investigation could be conducted for bosons, replacing the Slater determinants with Slater permanents.

The model uses a Hamiltonian $\hat{H} = \hat{\mathcal{T}} + \hat{\mathcal{V}}$. The one-body operator $\hat{\mathcal{T}}$ is the well known single-particle HO Hamiltonian

$$\hat{\mathcal{T}} = \frac{\hat{p}^2}{2m_p} + \frac{m_p \omega^2 \hat{x}^2}{2}$$

with eigenfunctions

$$\langle x | \phi_{\tilde{m}} \rangle = \phi_{\tilde{m}}(x) = \frac{1}{\sqrt{2^{\tilde{m}} \tilde{m}!}} \left(\frac{m_p \omega}{\pi \hbar} \right)^{\frac{1}{4}} e^{-\frac{x^2}{2}} H_{\tilde{m}} \left(\sqrt{\frac{m_p \omega}{\pi \hbar}} x \right),$$

using the Hermite polynomials $H_{\tilde{m}}(x) = (-1)^{\tilde{m}} e^{x^2} \frac{\partial^{\tilde{m}}}{\partial x^{\tilde{m}}} (e^{-x^2})$. The eigenvalues are

$$\lambda_{\tilde{m}} = \hbar \omega \left(\tilde{m} + \frac{1}{2} \right).$$

In this work, the lowest 5 basis states are used, with spin degeneracy, so that the basis states will be labeled $m \in \{1..M\}$, $M = 10$ corresponding to harmonic number $\tilde{m}_i = \lfloor \frac{m_i - 1}{2} \rfloor$ and spin $S_i = \frac{1}{2}(-1)^{m_i}$.

$\hat{\mathcal{V}}$ is a two-body operator, and is defined in spatial representation as

$$\begin{aligned} \langle m_1, m_2 | \hat{\mathcal{V}} | m_3, m_4 \rangle &= \\ &= \int_{-\infty}^{\infty} \int_{-\infty}^{\infty} dx' dx \phi_{\tilde{m}_1}(x) \phi_{\tilde{m}_2}(x') V(x, x') \phi_{\tilde{m}_3}(x) \phi_{\tilde{m}_4}(x') \delta_{S_1, S_3} \delta_{S_2, S_4} = \\ &= \left[V(x, x') = s \delta(x - x') \right] = \delta_{S_1, S_3} \delta_{S_2, S_4} s \int_{-\infty}^{\infty} dx \phi_{\tilde{m}_1}(x) \phi_{\tilde{m}_2}(x) \phi_{\tilde{m}_3}(x) \phi_{\tilde{m}_4}(x). \end{aligned}$$

Here, s is a interaction strength parameter, which can be negative for attractive interaction or positive for repulsive interaction. This delta interaction is used to model interactions between particles at close quarters.

A combined Hamiltonian tensor $H_{m_1 m_2 m_3 m_4}$ can be constructed as

$$\begin{aligned} H_{m_1 m_2 m_3 m_4} &= \delta_{\tilde{m}_1, \tilde{m}_3} \delta_{\tilde{m}_2, \tilde{m}_4} \frac{\hbar \omega \left(\tilde{m}_1 + \frac{1}{2} \right)}{N - 1} + \\ &+ \delta_{S_1, S_3} \delta_{S_2, S_4} s \int_{-\infty}^{\infty} dx \phi_{\tilde{m}_1}(x) \phi_{\tilde{m}_2}(x) \phi_{\tilde{m}_3}(x) \phi_{\tilde{m}_4}(x) \end{aligned}$$

using the reformulation of $\hat{\mathcal{T}}$ as a two-particle operator derived in [5].

2.1.2 States

In Hartree-Fock, the ground state $|\Psi^0\rangle$, labelled with an upper index 0 to signify ground state, is approximated with a Slater determinant $|\Psi_{HF}\rangle = |\varphi_1^0\rangle$,

$$|\varphi_1^0\rangle = \prod_{n=1}^N \left(\sum_{m=1}^M D_{m,n} a_m^\dagger \right) |-\rangle .$$

Here, a_m^\dagger is the creation operator to put a particle in state m in the vacuum $|-\rangle$. D is a semi-orthogonal ($M \times N$) matrix of coefficients, which are chosen through variation. D characterizes $|\varphi\rangle$ completely, and many properties of the state can be expressed as matrix operations on D , as described in section 2.1.3.

In [5], an expansion was discussed, where the ground state approximation was improved by adding more determinants $|\varphi_q^0\rangle$:

$$|\psi^0\rangle = \sum_q^Q f_q^0 |\varphi_q^0\rangle .$$

In order to maintain normality, this solution requires a vector $f_\bullet^0 = (f_1^0 \ f_2^0 \ \dots \ f_Q^0)$ of intra-state coefficients. Each time a new determinant is to be added, the previous f vector is scaled down by some factor $\sqrt{\aleph}$. In this thesis an arbitrarily chosen \aleph of 0.9 is used. If $|\varphi\rangle$ were orthogonal, this would correspond to keeping 90% of the old approximation, and the next coefficient would be easily found through Pythagoras: $f_Q^0 = \sqrt{1 - \aleph}$. Since the Slater determinants are non-orthogonal, the last f depends on the determinant overlaps $\mathbf{O}_{q_A q_B}^0 = \langle \varphi_{q_A}^0 | \varphi_{q_B}^0 \rangle$ and the previous $f_{<Q}^0 = (f_1^0 \ f_2^0 \ \dots \ f_{Q-1}^0)$:

$$f_Q^0 = -f_{<Q}^{0T} \mathbf{O}_{<Q Q}^0 + \sqrt{f_{<Q}^{0T} \left(\mathbf{O}_{<Q Q}^0 \mathbf{O}_{Q <Q}^0 - \mathbf{O}_{<Q <Q}^0 \right) f_{<Q}^0 + 1} .$$

This expression is derived in appendix A.1. \aleph is still in a sense a measure of how much is conserved, just not as straight-forward as in the orthogonal case.

As a next step, excited states are found through Gram-Schmidt orthogonalization. A pseudo state $|\psi^1\rangle$ (“pseudo” because it is turned into a state by orthogonalization) is found in the same way as $|\psi^0\rangle$, while continuously updating the inter-state coefficients c_0^1, c_1^1 so that $|\Psi^1\rangle = c_0^1 |\psi^0\rangle + c_1^1 |\psi^1\rangle$ is orthogonal to $|\Psi^0\rangle = |\psi^0\rangle$. More generally,

$$|\Psi^E\rangle = \sum_e^E c_e^E |\psi^e\rangle$$

with a triangular matrix of coefficients

$$c = \begin{pmatrix} c_0^0 & c_0^1 & \cdots & c_0^E \\ & c_1^1 & & \vdots \\ & & \ddots & c_e^E \\ 0 & & & c_E^E \end{pmatrix}$$

which is completely determined by the pseudo-state overlap $\mathbf{G}_{e_A e_B} = \langle \psi^{e_A} | \psi^{e_B} \rangle$ as derived in appendix A.2:

$$c_{<E}^E = -\mathcal{G}_{<E} c_E^E$$

$$c_E^E = \left(-\mathcal{G}^\top \mathbf{G}_{\bullet E} \right)^{-\frac{1}{2}}$$

with a column vector

$$\mathcal{G} = \begin{pmatrix} (\mathbf{G}_{<E<E})^{-1} \mathbf{G}_{<EE} \\ -1 \end{pmatrix}.$$

There is an $(E-1 \times E-1)$ matrix inversion involved in each update of the c matrix, which grows exponentially in time complexity. Luckily, one can reuse the previously determined $(\mathbf{G}_{<E-1<E-1})^{-1}$, in the *Bordering method*, only taking into account the added $E-1$ elements of \mathbf{G} . The new inverse is given from e.g. [3] as

$$\begin{pmatrix} \mathbf{A} & \vec{B} \\ \vec{B}^\top & d \end{pmatrix}^{-1} = \begin{pmatrix} \mathbf{A}^{-1} + \frac{1}{\alpha} \mathbf{A} \vec{B} \vec{B}^\top \mathbf{A} & -\frac{1}{\alpha} \mathbf{A} \vec{B} \\ -\frac{1}{\alpha} \vec{B}^\top \mathbf{A} & \frac{1}{\alpha} \end{pmatrix}$$

with $\alpha = d - \vec{B}^\top \mathbf{A} \vec{B}$.

In both f and c , a choice of phase is available for each of the coefficients as they are solutions to quadratic equations. The positive sign will be consistently chosen throughout this thesis, as in much of the literature, as it seems to have very little effect on the convergence of the search algorithm, or on the found states.

2.1.3 Properties of the Slater determinants

Some important properties of the Slater determinants can be expressed in terms of matrix operations on their defining coefficient matrices D , as follows: Because of the anti-commutation properties of the creation operator \hat{a}_m^\dagger , which enforce the Pauli principle,

$$\{\hat{a}_{m_1}^\dagger, \hat{a}_{m_2}\} = \delta_{m_1, m_2}$$

$$\{\hat{a}_{m_1}^\dagger, \hat{a}_{m_1}^\dagger\} = 0$$

$$\{\hat{a}_{m_1}, \hat{a}_{m_1}\} = 0$$

it can be shown, as is done in [8], that the determinant overlap

$$\mathbf{O}_{AB} = \langle \varphi_A | \varphi_B \rangle = \det \left(D_B^\top D_A \right),$$

that the density matrix is

$$\rho_{m_1 m_2}^{A B} = \frac{\langle \varphi_B | \hat{a}_{m_2}^\dagger \hat{a}_{m_1} | \varphi_A \rangle}{\langle \varphi_B | \varphi_A \rangle} = D_A \left(D_B^\top D_A \right)^{-1} D_B^\top,$$

and finally that the energy overlap

$$\mathbf{H}_{AB} = \langle \varphi_A | \hat{H} | \varphi_B \rangle = \mathbf{O}_{AB} \sum_{\substack{m_1, m_2, \\ m_3, m_4}} \rho_{m_1 m_2}^{A B} \rho_{m_3 m_4}^{A B} (H_{m_1 m_3 m_4 m_2} - H_{m_1 m_3 m_2 m_4}).$$

2.2 Gradient descent

The *variational principle* gives that an operator’s eigenvectors are minimum coordinates to its expectation value,

$$\partial \frac{\langle \Psi | \hat{H} | \Psi \rangle}{\langle \Psi | \Psi \rangle} = 0,$$

and those minima can be found by stepping the D matrix in the opposite direction of the energy gradient, using a gradient descent method as described below.

Gradient descent is the multi-dimensional equivalent of attempting to find the lowest point in a landscape by walking downhill along the steepest possible path. The method is often used in artificial neural networks, and several methods have been developed in order to do it quickly and efficiently. The naïve idea, “walk along the steepest path until the slope is 0” has a number of problems:

- One could be far from a minimum, and if the descent rate is constant, it can take a long time to get there.
- If finding the slope is computationally expensive, as is the case in this method, it would be beneficial to set a course and maintain it, rather than re-evaluate the gradient at each step.
- This method is prone to getting stuck in local minima – with a small hurdle in the way of true minima. While there is no way to guarantee that a global minimum was reached without a complete analytical description of the landscape, there are methods that are much more resilient to local minima.

A number of gradient descent methods were tried, and the most interesting ones were *Proportional descent*, *Rprop* and *Stiefel descent*.

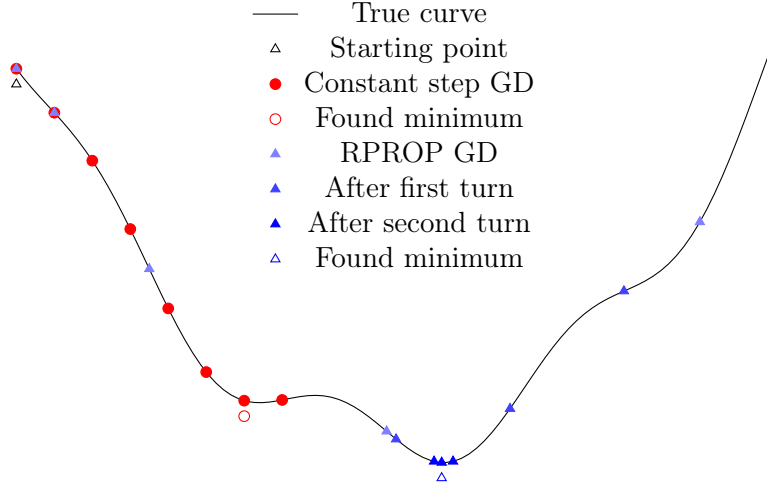


Figure 1: Demonstration of problems with naïve gradient descent (in 1 dimension).

2.2.1 Proportional descent

In [5] a simple descent method was used where the steps were proportional to the gradient, and the course was held until the energy started rising. This was repeated until the energy was updated a small enough amount. This proportional descent is suitable for a certain type of landscape, where points far from the minimum have steep gradients, and the gradient converges simply towards the minimum. For other landscapes, it can end up spending long time leaving low-gradient but high-energy points, and it is fairly sensitive to local minima.

2.2.2 Rprop

In Rprop (Resilient propagation), the step length for each matrix element is decided by whether or not the sign of the gradient's corresponding element changes, but not by the magnitude of the gradient. That way, after a given number of steps each element is likely to be at a value where its corresponding gradient sign keeps flipping, meaning a minimum. D is changed by an update matrix U , the elements of which are scaled by experimentally determined η^+ or η^- in each step, depending on whether the sign of the gradient flipped that step:

$$\eta_{m,n}^k = \begin{cases} \eta^+ = 1.4 & \frac{\partial \mathcal{E}}{\partial D_{m,n}^{k-1}} \cdot \frac{\partial \mathcal{E}}{\partial D_{m,n}^k} > 0 \\ \eta^- = 0.5 & \frac{\partial \mathcal{E}}{\partial D_{m,n}^{k-1}} \cdot \frac{\partial \mathcal{E}}{\partial D_{m,n}^k} < 0 \end{cases}$$

$$U_{m,n}^{k+1} = -\text{sgn}\left(\frac{\partial \mathcal{E}}{\partial D_{m,n}^k}\right) \eta_{m,n}^k U_{m,n}^k$$

$$D_{m,n}^{k+1} = D_{m,n}^k + U_{m,n}^{k+1}$$

2.2.3 Stiefel descent

In Rprop and other common descent methods, D needs to be orthogonalized occasionally, to maintain its semi-orthogonality. Since one element of each of the N columns is needed to normalize the column, and one extra element per column to the left is needed for orthogonality, $\frac{1}{2}N(N+1)$ degrees of freedom are removed. In effect the determinants are not really $M \times N = 40$ -dimensional, but rather $N \times (M - \frac{1}{2}(N+1)) = 30$, and any descent along those 10 extra dimensions is wasted work.

There is, however, a way to do gradient descent while inherently maintaining that semi-orthogonality. It involves projecting the gradient on a tangent space to the Stiefel manifold, and forming a single parameter search curve along the manifold. Since every point on the curve is a semi-orthogonal matrix, any D chosen from it will be too, and does not need to be orthogonalized. This descent method is described in [1]. In theory, this could save $\mathcal{O}(N^2)$ in computation, and the more particles are being considered, the larger the savings.

The general idea is to form a search path

$$Y(\tau) = \left(\mathbb{1} + \frac{\tau}{2}A \right)^{-1} \left(\mathbb{1} - \frac{\tau}{2}A \right) D_\star$$

where

$$A = \nabla_{D_\star} \mathcal{E} D_\star^\top - D_\star (\nabla_{D_\star} \mathcal{E})^\top$$

which can be shown to be a curve on the manifold in the opposite direction of $\nabla_{D_\star} \mathcal{E}$. $\tau \in \mathbb{R}$ is adjusted by some common descent method, just as if it were a $1D$ gradient descent.

The most time consuming part of this method is the inversion of a $M \times M$ -matrix, but according to the Sherman-Morrison-Woodbury theorem there is a way to simplify this type of inversion to an inversion of an $2N \times 2N$ -matrix, which is a large discount if the number of particles N is sufficiently smaller than the number of basis harmonics $\frac{M}{2}$.

2.3 Gradients

Initially, the gradient of the energy functional was found numerically, as

$$(\nabla_{D_\star} \mathcal{E})_{m,n} \approx \frac{\mathcal{E}(D_\star + \varepsilon \mathbf{J}_{(m,n)}) - \mathcal{E}(D_\star - \varepsilon \mathbf{J}_{(m,n)})}{2\varepsilon}$$

for some small ε , with the single-element matrix $\mathbf{J}_{(m,n)}$.

Calculating this gradient for each of 40 elements means 80 calculations of the energy, which itself is quite an expensive operation. Using matrix calculus, however, an analytical derivative can be found, which is more similar to the energy functional itself in complexity. The expression below is derived

in appendix B.

$$\begin{aligned} \frac{\partial \mathcal{E}}{\partial D_\star} &= 2c_E^E \left(\sum_{q_A, e_A} W_A \right) \frac{\partial f_\star}{\partial D_\star} + c_E^E f_\star \sum_{q_A, e_A} \mathcal{D}_A \left(2W_A \mathbb{1}_M + \right. \\ &\quad \left. + c_{e_A}^E f_A \mathbf{O}_{A^\star} \left(\sum_{m_1, m_2} \rho_{m_1 m_2}^{A^\star} \bar{\bar{H}}_{\bullet \bullet m_1 m_2} \right) (\mathbb{1}_M - \rho^{\star A}) \right) \end{aligned}$$

with

$$\begin{aligned} W_A &= c_{e_A}^E f_A \left(\mathbf{H}_{A^\star} - \varepsilon \mathbf{O}_{A^\star} \sum_{q_B, e_B} \mathbf{G}^i_{e_A e_B} f_B \sum_{q_C, e_C} c_{e_C}^E f_C \mathbf{H}_{C_B} \right), \\ \frac{\partial f_\star}{\partial D_\star} &= \left(\frac{\frac{1}{\mathbf{o}_{\star\star}} \left(f_{<Q}^{E\top} \left(2\mathbf{O}_{<Q}^E \mathbf{O}_{<Q}^E f_\star - \mathbf{O}_{<Q}^E \mathbf{O}_{<Q}^E f_{<Q}^E \right) + 1 \right) \mathcal{D}_\star \mp f_\star \sum_q f_q^E \mathbf{O}_{qQ}^{EE} \mathcal{D}_q^E}{\sqrt{\frac{1}{\mathbf{o}_{\star\star}} \left(f_{<Q}^{E\top} \left(\frac{\mathbf{O}_{<Q}^E \mathbf{O}_{<Q}^E \mathbf{O}_{<Q}^{EE}}{\mathbf{o}_{\star\star}} - \mathbf{O}_{<Q}^E \mathbf{O}_{<Q}^E \right) f_{<Q}^E + 1 \right)}} \right) \end{aligned}$$

and

$$\mathcal{D}_A = \left(D_A^\top D_\star \right)^{-1} D_A^\top.$$

This derivative is in numerator layout, so for gradient descent was used $\nabla_{D_\star} \mathcal{E} = \left(\frac{\partial \mathcal{E}}{\partial D_\star} \right)^\top$.

A similar expression was derived in [7], but for a slightly different model, and only for the ground state.

2.4 Configuration Interaction

In configuration interaction, the Schrödinger equation is solved by numerical diagonalization of the Hamiltonian matrix in a given basis of Slater determinants. Full CI uses a basis of determinants that spans the full space of many-body states, meaning diagonalization of, at best, a $\binom{M}{N} \times \binom{M}{N}$ matrix. This gives an exact solution of the SE, but matrix diagonalization is time intensive, and the matrix grows combinatorially with the model space.

For most applications, however, only the first few excited states matter. Finding Slater determinants that span a low-energy subspace of the full many-body state space is desirable, as it leads to quicker diagonalization without loss of accuracy in the important eigenvalues. For truncated CI using the basis of determinants found using the method described in this thesis, the generalized eigenvalue problem

$$\mathbf{H}\Phi = \mathbf{\Lambda}\mathbf{O}\Phi$$

is solved. The found Φ is a matrix of eigenvectors, and $\mathbf{\Lambda}$ is a diagonal matrix of eigenvalues. These eigenvalues are approximations of the solutions to the SE.

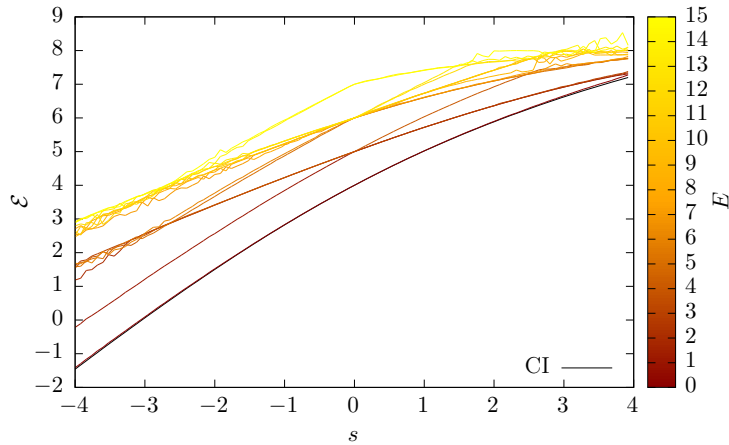


Figure 2: Ground and $E = 15$ first excited levels of $N = 4$ particles in a harmonic oscillator, using $Q = 10$ determinants per state.

3 Results

3.1 Gradients

As expected, the analytical calculations of the gradient took a fraction of the time required for numerical derivation. A code performance profile shows an improvement of about 20 times. Because the gradient accounts for 99% of a typical run time for Rprop with numerical gradient, this means huge savings.

To validate the analytical gradient, a random set of determinants were generated and the numerical and analytical gradients at that random point were compared. Statistical analysis of the difference between the individual elements, as well as ocular inspection of the gradients (fig. 3), confirm the formula.

3.2 Descent methods

Out of the tried descent methods Rprop turned out to be the fastest by far, followed by Stiefel and lastly proportional descent. A majority of the run time for Stiefel descent is unsurprisingly spent doing matrix inversion. With larger model spaces, the result might be different, but for few ($N \approx 2..5$) particles and this number of basis states ($M = 10$) Rprop has the speed advantage. Comparing runs of the descent methods of roughly equal time, Rprop has time to add more determinants, and the accuracy and reliability is therefore increased.

3.3 Accuracy

As in [5], accuracy in the ground state could be assessed through comparison with the exact CI solution. The excited states were mainly judged by intuitive physical reasoning (below) and by the “smoothness” of their curves. Figures 4

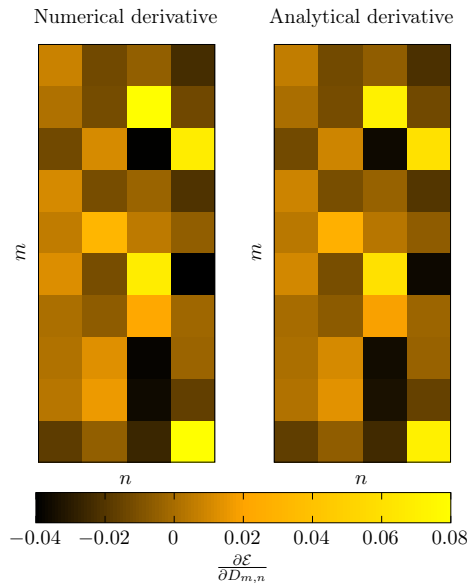


Figure 3: Example of the similarity between analytical and numerical derivative.

and 5 show the calculated energies as a function of interaction strength for four particles in a harmonic oscillator potential. There is a clearly visible improvement in accuracy going from $Q = 1$ to 7 determinants per state.

Three different types of errors can be distinguished in these two plots:

- *Inaccuracy*, due to inherent limitations in the model. The difference between the ground state and the full CI solution which is seen for large interaction strengths in fig. 4 is an example of this. A superposition of Slater determinants cannot solve the N body problem exactly, but this error can be reduced down to a limit by increasing the number of determinants.
- *State order swapping*, where two states have switched place. Here, a local minimum has been found instead of the global minimum, but it is still a physical state, and in the space of states orthogonal to this local minimum and all previous the real global minimum is easy enough to find for the next iteration. These problems can easily be solved by a simple sorting operation, and will disappear entirely in a subsequent CI calculation.
- *State mixing*, Here, the same error has been made as in the order swapping case, but some determinants correspond to one physical state and some to the other, causing the energy lines to appear to meet halfway. This problem arises when the states are near each other in the search space, and is in fact made worse by adding more determinants. A possible solution is occasional gradient descent on f , making sure

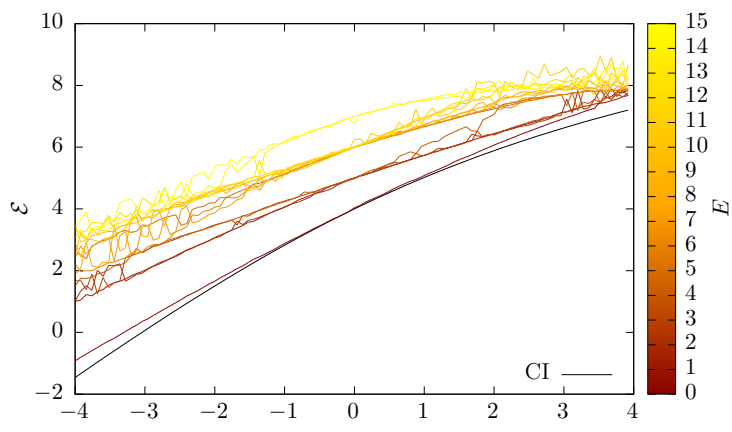


Figure 4: $Q = 1$ determinant/state.

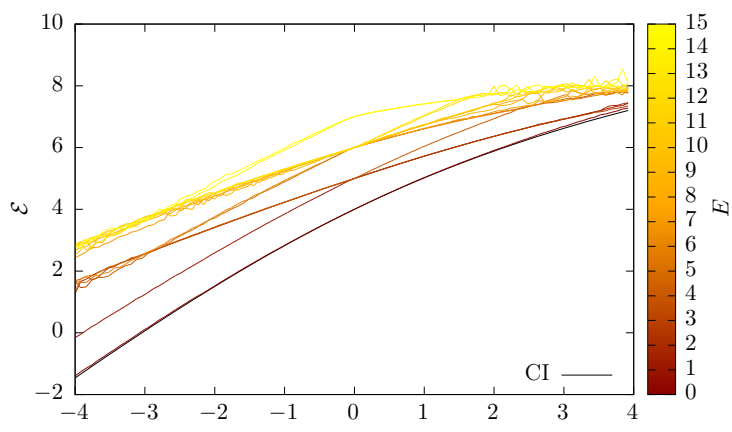


Figure 5: $Q = 7$ determinants/state.

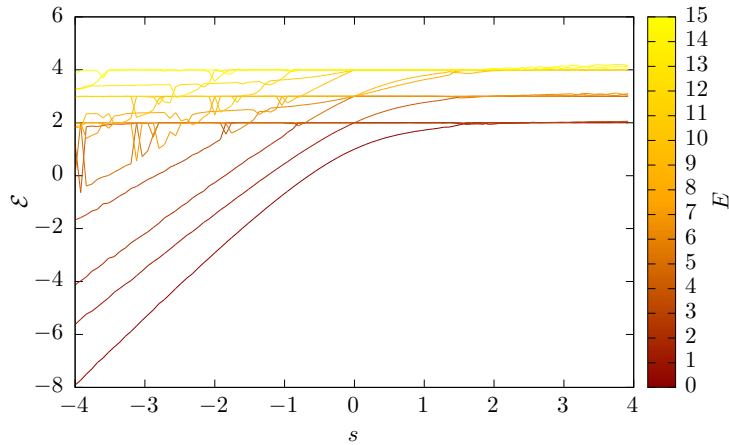


Figure 6: $N = 2$ interacting particles.

that the contribution from the higher state is given a zero amplitude.

This method is limited by the fact that errors are accentuated for each excitation: The ground state is almost-physical, the first excited state is the lowest energy state that is orthogonal to the ground state, meaning that it is (possibly) a worse approximation than the ground state was. Each successive excitation includes and compounds the error from each previous.

3.4 Number of particles

The default testing case in this thesis uses $N = 4$ particles, but this can be altered (and would ideally be expanded into the nuclear physics range). Figure 6 shows the energy for 2 particles, fig. 7 for 3, and fig. 8 for 5. The states in these three figures have been approximated with $Q = 10$ determinants per layer. As will be discussed in section 3.7, these results match the expectations well.

3.5 Time complexity

By timing the program, some analysis could be made of the time complexity of the method. No exact description of asymptotic behavior is possible from this small range of model spaces, but as is shown in fig. 9, the timing of individual runs shows an exponential behavior for increases in number of particles N and number of determinants Q , while an increase in number of excited states E scales the time quadratically.

3.6 Configuration interaction

While a bit outside the scope of this thesis, fig. 10 demonstrates the improvement in doing CI with the found basis. Here, $E = 4$ states represented

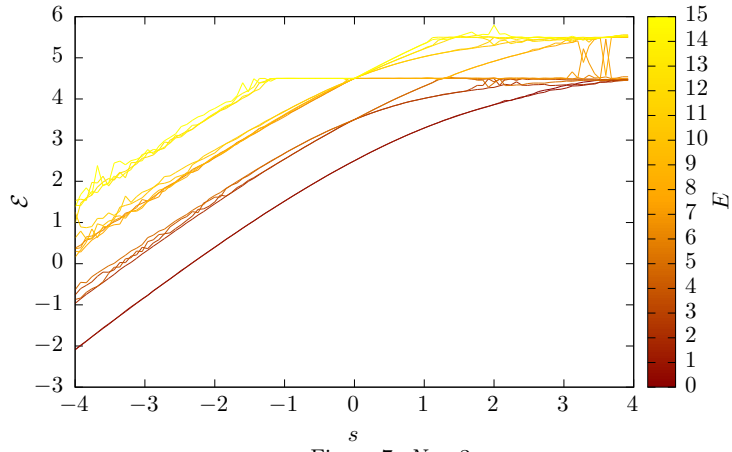


Figure 7: $N = 3$.

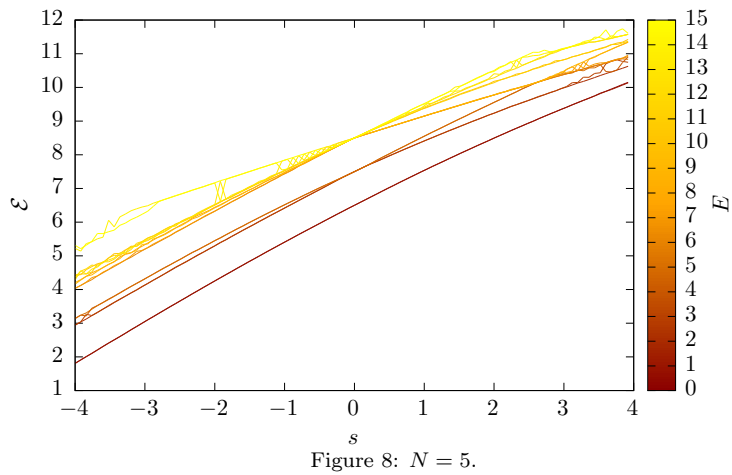


Figure 8: $N = 5$.

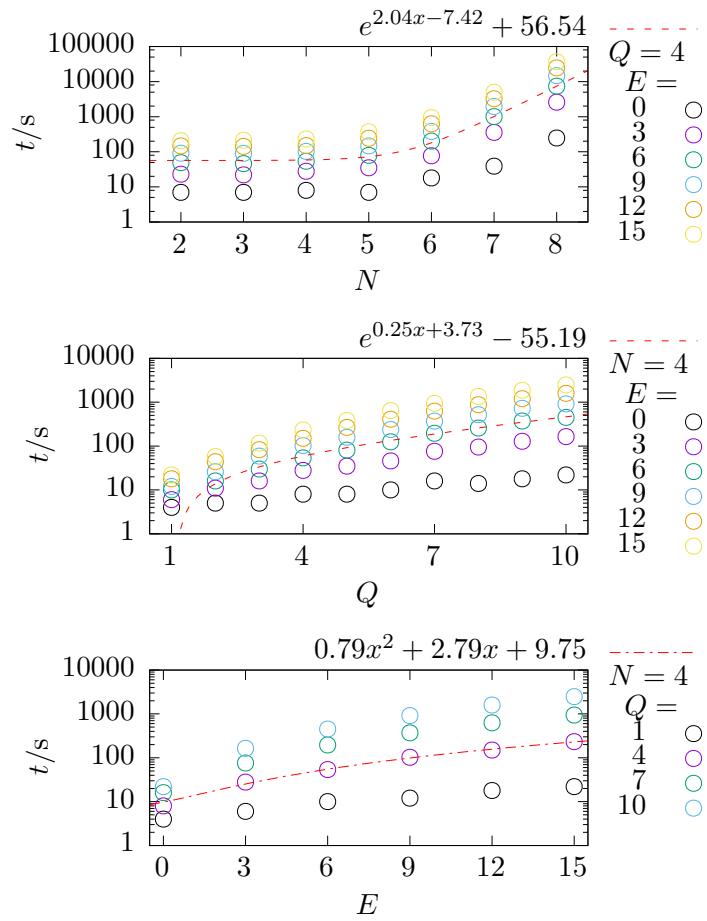


Figure 9: Time in seconds (logarithmic) for runs with different number of particles N (top), number of determinants per state Q (middle) and number of excited states E (bottom).

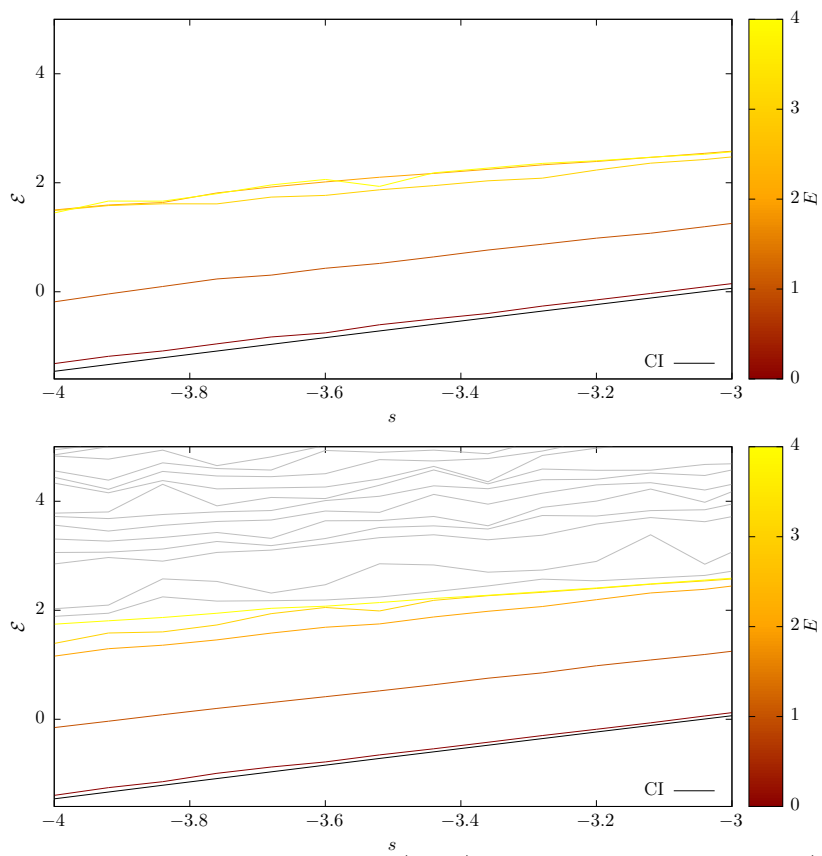


Figure 10: Truncated CI on found basis (below), compared to the found energies (above).

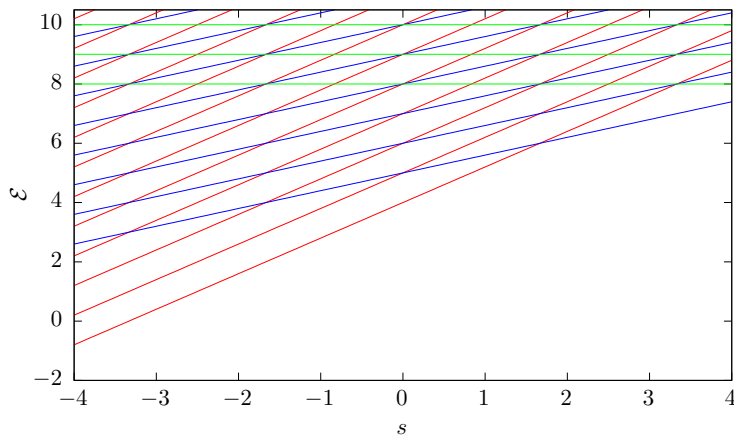


Figure 11: Schematic image of tangents to the energy curves.

by $Q = 5$ determinants each are calculated and shown in the upper plot. The plot below it shows the eigenvalues of the corresponding Hamiltonian matrix. Of course, as $Q \times (E + 1) = 25$ determinants are used, that is also the number of eigenvalues. However, since determinants that describe the first $E + 1$ states were intentionally chosen, the higher eigenvalues (in gray) are not meaningful.

As expected the ground state (in dark red) is notably closer to the exact full CI solution in the lower picture than in the higher, and the excited states are smoother.

3.7 Physical interpretation of results

This subsection contains a physical interpretation of these results, as a description of a few fermions trapped in a harmonic oscillator potential. These results are not groundbreaking, but serve as a proof of concept.

Figure 11 shows a possible intuitive interpretation of the calculated energies for 4 particles. The red lines correspond to *modes* where the particles lie in two pairs, while the blue are ones with one pair and two independent particles and green are ones without pairs. Therefore, the slope $\frac{dE}{ds}$ of the red lines is about twice that of the blue, and 0 for the green. These straight lines are the tangents at $s = 0$. In the simulations and in physical reality, the states are free to combine in less straight-forward ways, giving a higher slope for large attractive potential, and a lower slope for large repulsive potential.

The *Hellman-Feynman theorem*, proven e.g. in [2] provides a motivation for this picture:

$$\begin{aligned} \frac{\partial \mathcal{E}}{\partial s} &= \frac{\partial}{\partial s} \langle \Psi(s) | \hat{\mathcal{T}} + s \hat{\mathcal{V}} | \Psi(s) \rangle = [\text{Hellman-Feynman}] = \\ &= \langle \Psi | \frac{\partial}{\partial s} (\hat{\mathcal{T}} + s \hat{\mathcal{V}}) | \Psi \rangle = \langle \hat{\mathcal{V}} \rangle \end{aligned}$$

where $\hat{V} = \frac{\hat{Y}}{s}$ has an expectation value \propto the number of particle pairs in the state $|\Psi\rangle$. The changes in the number of pairs is what causes the bending of the energy curves.

Using the diagonal values of the density matrix and reasoning on the slopes of the energy curve (using e.g. fig. 12), one can figure out an intuitive description of which harmonics the particles actually occupy, and how. These descriptions are displayed in table 1. In a sense, the construction of the table is the opposite process of configuration interaction theory, where basis determinants are chosen by considering the excitations of singles and pairs, followed by diagonalization. Many of the configurations are degenerate, meaning that there is more than one configuration that leads to the same energy. In table 1, linewise degenerate states (which have the same or similar energy for all s) are grouped by rules. At values of s where energy lines cross, the energies are extra degenerate. Notably, at $s = 0$ many such pointwise degeneracies appear.

When the number of particles is increased, the single-particle energy sum ($\mathcal{E}_{(s=0)}$) goes up proportionally. Odd numbers of particles give rise to degenerate ground states, having a choice of spin for the odd particle. With even N , the ground state (for low enough s) has pairs of particles in the first $\frac{N}{2}$ harmonics, and there is only one such configuration.

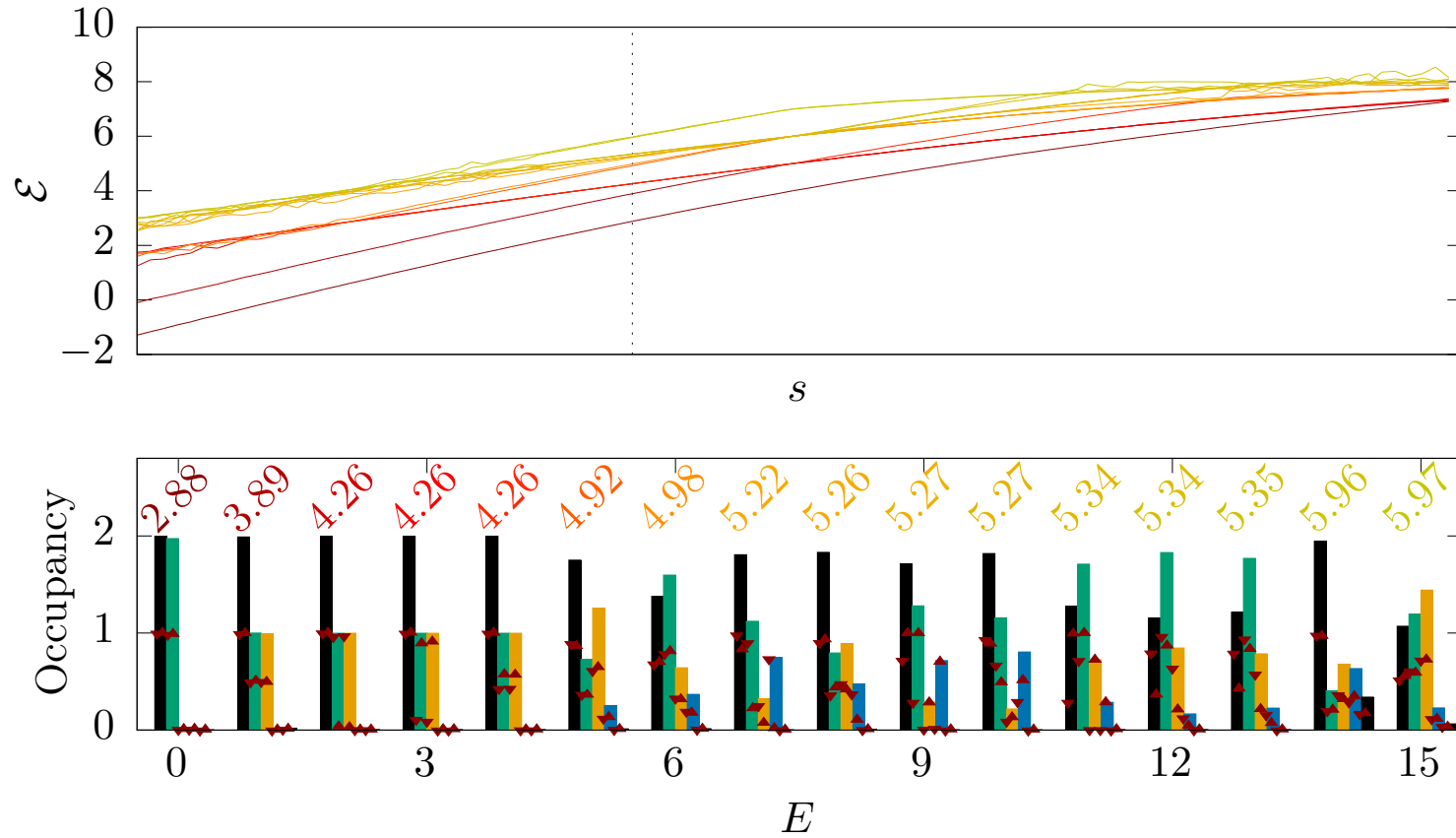


Figure 12: The energies for $N = 4$ particles (above) and the diagonal values of the density matrix (below) at $s = -1$ (marked above with a dashed line). Each group of bars in the lower plot corresponds to a state, and each bar in the group gives the occupancy of a basis state ($\tilde{m} = 1 \dots 5$). Each bar has two arrows, showing the spin distribution. To aid with interpretation, each state's energy and color code is given above the bar group.

4 Discussion

4.1 Conclusion

The described iterative post-Hartree-Fock method can reliably calculate approximations to the ground and first few excited states of an N body quantum mechanical 1D harmonic oscillator, and the found Slater determinants form a basis for a low-energy space for configuration interaction. The time complexity appears to grow exponentially with model size, which potentially makes it faster and more feasible for large systems than full CI which grows factorially. Just how large systems are feasible is hard to say without large scale benchmarking.

4.2 Extensions

In order to use this method for nuclear or atomic physics, it needs to be implemented with a more realistic model, like a 3D harmonic oscillator. This adaptation is in principle just a matter of extending the Hamiltonian tensor.

The model space needs to be expanded into much higher N , which will require optimizations. A couple of possibilities arise: Instead of taking the positive sign for every choice of c and f , a phase could be recorded for each such choice, allowing the descent to choose whichever sign gives the lower energy. This could possibly help shorten the time to convergence. Another impactful change would be to use more intelligently chosen initial D matrices instead of just randomizing. For instance, determinants within a state would be expected to be similar, so using the previously found D , with some noise, as a starting point to find the next one could be advantageous. A well implemented propagation method on the f vectors could save some time by reducing the number of determinants required for accuracy. With some extensive benchmarking, it might be possible to find an optimal \aleph , or some other method of re-scaling the determinants.

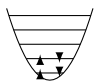
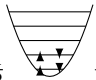
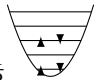
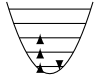
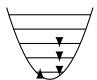
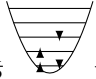
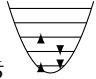
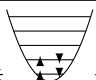
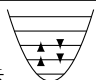
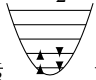
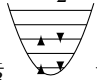
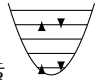
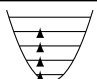
One possible way of increasing the speed and stability of this method is to view the choice of inter-state coefficients c not as a Gram-Schmidt orthogonalization, but as a Cholesky decomposition, where

$$\mathbf{G} = LL^T$$

and $c = L^{-T}$, which should be a quick inversion to perform because of the triangular structure of L .

In order to prove the feasibility of this method, it would need to be compared, in accuracy and time, with some implementation of full CI on the same system.

Table 1: The first states at $s = -1$ for $N = 4$ particles. As s changes, so will the ordering and the energy. The configurations will also be decreasingly pure as $|s|$ increases, the table displays the idealized $s = 0$ representation. For some states, the density matrix diagonals and slopes are not enough information to figure out an intuitive occupancy description or one with few enough components to fit.

E	Occupancy	$\langle \hat{T} \rangle$	Number of pairs	$\mathcal{E}/\hbar\omega$
0		4	2	2.88
1	$\frac{1}{2}$  + $\frac{1}{2}$ 	5	2	3.89
2		5	1	
3		5	1	4.26
4	$\frac{1}{2}$  + $\frac{1}{2}$ 	5	1	
5	$\frac{1}{2}$  + $\frac{1}{2}$ 	6	2	
6	$\frac{1}{3}$  + $\frac{1}{3}$  + $\frac{1}{3}$ 	6	2	4.92
	\vdots			
		8	0	8

References

- [1] Dimitri P. Bertsekas. *Constrained Optimization and Lagrange Multiplier Methods*. Athena Scientific, 1996.
- [2] R. P. Feynman. “Forces in Molecules”. In: *Physical Review* 56 (Aug. 1939), pp. 340–343. DOI: [10.1103/PhysRev.56.340](https://doi.org/10.1103/PhysRev.56.340).
- [3] Roger A. Horn and Charles R. Johnson. *Matrix Analysis*. 2nd. New York, NY, USA: Cambridge University Press, 2012. ISBN: 9780521548236.
- [4] K. B. Petersen and M. S. Pedersen. *The Matrix Cookbook*. Version 20121115. Kongens Lyngby, Nov. 2012. URL: <http://www2.imm.dtu.dk/pubdb/p.php?3274>.
- [5] Claes Rogius Svensson. “Variational approach to the many-body problem with error estimation”. Eng. Student Paper. MA thesis. Lund University, Faculty of Engineering, 2018.
- [6] K.W. Schmid. “On the use of general symmetry-projected Hartree-Fock-Bogoliubov configurations in variational approaches to the nuclear many-body problem”. In: *Progress in Particle and Nuclear Physics* 52.2 (2004), pp. 565–633. ISSN: 0146-6410. DOI: <https://doi.org/10.1016/j.pnpnp.2004.02.001>. URL: <http://www.sciencedirect.com/science/article/pii/S0146641004000134>.
- [7] N. Shimizu et al. “New-generation Monte Carlo shell model for the K computer era”. In: *Progress of Theoretical and Experimental Physics* 2012.1, 01A205 (Sept. 2012), 01A205. DOI: [10.1093/ptep/pts012](https://doi.org/10.1093/ptep/pts012). arXiv: [1207.4554](https://arxiv.org/abs/1207.4554) [nucl-th].
- [8] Yutaka Utsuno et al. “Efficient computation of Hamiltonian matrix elements between non-orthogonal Slater determinants”. In: *Computer Physics Communications* 184.1 (2013), pp. 102–108. ISSN: 0010-4655. DOI: <https://doi.org/10.1016/j.cpc.2012.09.002>. URL: <http://www.sciencedirect.com/science/article/pii/S0010465512002883>.

A Coefficients

A.1 Method for intra-state coefficients

The latest intra-state coefficient f_\star is chosen to make sure that the pseudo-state $|\psi^E\rangle$ is normalized. Because the Slater determinants are not orthogonal, f_\star will depend on the previously chosen $f_{<Q}^E$ and the determinant overlaps $\langle\varphi_A|\varphi_B\rangle = \mathbf{O}_{AB}$:

$$\begin{aligned}
& \langle\psi^E|\psi^E\rangle = 1 \\
& = \sum_{q_A, q_B} f_{q_A}^E f_{q_B}^E \mathbf{O}_{q_A q_B}^{E E} = f_\star \sum_{q_B} f_{q_B}^E \mathbf{O}_{q_A q_B}^{E E} + \sum_{q_A}^{Q-1} f_{q_A}^E \sum_{q_B} f_{q_B}^E \mathbf{O}_{q_A q_B}^{E E} \\
& = (f_\star)^2 \mathbf{O}_{\star\star} + 2f_\star \sum_q^{Q-1} f_q^E \mathbf{O}_q^{EEQ} + \sum_{q_A, q_B}^{Q-1} f_{q_A}^E f_{q_B}^E \mathbf{O}_{q_A q_B}^{E E} \\
& \implies (f_\star)^2 + \mathcal{P} f_\star + \mathcal{Q} = 0 \text{ where} \\
& \mathcal{P} = \frac{2}{\mathbf{O}_{\star\star}} \sum_q^{Q-1} f_q^E \mathbf{O}_q^{EEQ}, \quad \mathcal{Q} = \frac{1}{\mathbf{O}_{\star\star}} \left(\sum_{q_A, q_B}^{Q-1} (f_{q_A}^E f_{q_B}^E \mathbf{O}_{q_A q_B}^{E E}) - 1 \right) \\
& \implies f_\star = -\frac{\mathcal{P}}{2} \pm \sqrt{\left(\frac{\mathcal{P}}{2}\right)^2 - \mathcal{Q}} = -\frac{1}{\mathbf{O}_{\star\star}} \sum_q^{Q-1} f_q^E \mathbf{O}_q^{EEQ} \\
& \pm \sqrt{\frac{1}{(\mathbf{O}_{\star\star})^2} \sum_{q_A, q_B}^{Q-1} f_{q_A}^E f_{q_B}^E \mathbf{O}_{q_A Q}^{E E} \mathbf{O}_{q_B Q}^{E E} - \frac{1}{\mathbf{O}_{\star\star}} \left(\sum_{q_A, q_B}^{Q-1} (f_{q_A}^E f_{q_B}^E \mathbf{O}_{q_A q_B}^{E E}) - 1 \right)}. \tag{A1}
\end{aligned}$$

The positive sign is chosen.

Assuming normality within the Slater determinants, $\mathbf{O}_{AA} = 1$,

$$f_\star = -f_{<Q}^{E\top} \mathbf{O}_{<Q Q}^{E E} + \sqrt{f_{<Q}^{E\top} \left(\mathbf{O}_{<Q Q}^{E E} \mathbf{O}_{Q <Q}^{EE} - \mathbf{O}_{<Q <Q}^{E E} \right) f_{<Q}^E + 1}. \tag{A2}$$

A.2 Method for inter-state coefficients

The inter-state coefficients c_\bullet^E must be chosen so as to make $|\Psi\rangle$ orthogonal:

$$\langle\Psi^e|\Psi^E\rangle = \delta_{e,E}.$$

Keeping in mind that c is upper-triangular, so $c_e^E = 0$ if $e > E$:

$$\begin{aligned}
\langle\Psi^e|\Psi^E\rangle_{\{e < E\}} = 0 & = \left(c_{<E}^{e\top} \ 0 \right) \begin{pmatrix} \mathbf{G}_{<E <E} & \mathbf{G}_{<E E} \\ \mathbf{G}_{E <E} & \mathbf{G}_{EE} \end{pmatrix} c_\bullet^E = \\
& = c_{<E}^{e\top} \left(\mathbf{G}_{<E <E} c_{<E}^E + \mathbf{G}_{<E E} c_E^E \right).
\end{aligned}$$

Since this equation must hold at $e = 0$, with $c_0^0 \neq 0, c_{>0}^0 = 0$, the first element of the parenthesis must be 0. By induction,

$$\begin{aligned} (\mathbf{G}_{<E<E}c_{<E}^E + \mathbf{G}_{<EE}c_E^E) &= 0 \\ c_{<E}^E &= -\mathbf{G}_{<E<E}^i \mathbf{G}_{<EE}c_E^E = -\mathcal{G}_{<E}c_E^E. \end{aligned}$$

This can be replaced into

$$\begin{aligned} 1 &= \langle \Psi^E | \Psi^E \rangle = c_{<E}^{E\top} \mathbf{G}_{<E<E}c_{<E}^E + 2c_{<E}^{E\top} \mathbf{G}_{<EE}c_E^E + (c_E^E)^2 \mathbf{G}_{EE} = \\ &= \left(\mathcal{G}_{<E}^\top \overbrace{\mathbf{G}_{<E<E} \mathbf{G}_{<E<E}^i \mathbf{G}_{<EE}}^{=1} - 2\mathcal{G}_{<E}^\top \mathbf{G}_{<EE} + \mathbf{G}_{EE} \right) (c_E^E)^2 \\ &\implies c_E^E = \pm \left(\mathbf{G}_{EE} - \mathcal{G}_{<E}^\top \mathbf{G}_{<EE} \right)^{-\frac{1}{2}} = \pm \left(-\mathcal{G}^\top \mathbf{G}_{\bullet E} \right)^{-\frac{1}{2}}. \end{aligned}$$

Again, the positive sign is chosen.

B Analytic derivatives of the energy functional

The latest D -matrix D_Q^E is shortened D_* , and states pertaining to it will be labelled with Q^E or $*$, whereas arbitrary states will be labelled q_A^E and q_B^E or A and B .

This section uses differential identities and methods from [4]. Now,

$$\partial\mathcal{E} = \partial \langle \Psi^E | \hat{H} | \Psi^E \rangle = \partial \sum_{\substack{q_A, q_B, \\ e_A, e_B}} c_{e_A}^E c_{e_B}^E f_A f_B \langle \varphi_A | \hat{H} | \varphi_B \rangle .$$

This becomes

$$\partial\mathcal{E} = \sum_{\substack{q_A, q_B, \\ e_A, e_B}} c_{e_A}^E c_{e_B}^E \mathbf{H}_{AB} (f_A \partial(f_B) + f_B \partial(f_A)) + f_A f_B \mathbf{H}_{AB} (c_{e_A}^E \partial(c_{e_B}^E) + c_{e_B}^E \partial(c_{e_A}^E)) + c_{e_A}^E c_{e_B}^E f_A f_B \partial(\mathbf{H}_{AB}) .$$

29

These differentials can all be reduced to an expression like $\partial\mathcal{E} = \text{tr}(\mathbf{X}\partial D_*) \implies \frac{\partial\mathcal{E}}{\partial D_*} = \mathbf{X}$ as such:

$$\begin{aligned} \partial\mathbf{O}_{AB} &= \partial \langle \varphi_{q_A}^{e_A} | \varphi_{q_B}^{e_B} \rangle = \partial \det \left(D_B^\top D_A \right) = \mathbf{O}_{AB} \text{tr} \left(\left(D_B^\top D_A \right)^{-1} D_B^\top \partial D_A + \left(D_A^\top D_B \right)^{-1} D_A^\top \partial D_B \right) \\ \frac{\partial\mathbf{O}_{AB}}{\partial D_*} &= \mathbf{O}_{AB} \left(\delta_{A,*} (D_B^\top D_*)^{-1} D_B^\top + \delta_{B,*} (D_A^\top D_*)^{-1} D_A^\top \right) = \\ &= \mathbf{O}_{AB} (\delta_{A,*} \mathcal{D}_B + \delta_{B,*} \mathcal{D}_A) \end{aligned}$$

where $\mathcal{D}_A = (D_A^\top D_*)^{-1} D_A^\top$ will prove to be a common enough construction as to warrant a shorthand.

The derivative of f_\star by necessity uses the longer version of the expression, eq. (A1), because the assumption required for the shorter version eq. (A2), that the determinants are normalized, does not hold for arbitrary variation on the elements of D_\star . In short, if $\frac{\partial \mathbf{O}_{AA}}{\partial D_\star}$ was 0 the shorter expression could be used, but it isn't.

$$\begin{aligned} \frac{\partial f_A}{\partial D_\star} &= \delta_{A,\star} \left(\left(-\frac{1}{2} + \frac{\mathcal{P}}{4\sqrt{(\frac{\mathcal{P}}{2})^2 - \mathcal{Q}}} \right) \frac{\partial \mathcal{P}}{\partial D_\star} - \frac{1}{2\sqrt{(\frac{\mathcal{P}}{2})^2 - \mathcal{Q}}} \frac{\partial \mathcal{Q}}{\partial D_\star} \right) = \\ &= \delta_{A,\star} \left(\frac{\frac{1}{\mathbf{o}_{**}} \left(f_{<Q}^{E\Gamma} \left(2\mathbf{O}_{<QQ}^{E\ E} f_\star - \mathbf{O}_{<Q<Q}^{E\ E} f_{<Q}^E \right) + 1 \right) \mathcal{D}_\star - f_\star \sum_q f_q^E \mathbf{O}_{qQ}^{EE} \mathcal{D}_q^E}{\sqrt{\frac{1}{\mathbf{o}_{**}} \left(f_{<Q}^{E\Gamma} \left(\frac{\mathbf{O}_{<QQ}^{E\ E} \mathbf{O}_{Q<Q}^{EE} - \mathbf{O}_{<Q<Q}^{E\ E} \right) f_{<Q}^E + 1 \right)}} \right) \end{aligned}$$

30

$$\begin{aligned} \partial \mathbf{G}_{e_A e_B} &= \partial \langle \psi^{e_A} | \psi^{e_B} \rangle = \sum_{q_A, q_B}^Q (f_A f_B \partial(\mathbf{O}_{AB}) + \mathbf{O}_{AB} (f_A \partial(f_B) + f_B \partial(f_A))) = \\ &= \sum_{q_A, q_B}^Q (f_A f_B \mathbf{O}_{AB} \text{tr}((\mathcal{D}_B \partial D_A + \mathcal{D}_A \partial D_B)) + \mathbf{O}_{AB} (f_A \partial(f_B) + f_B \partial(f_A))) \\ \frac{\partial \mathbf{G}_{e_A e_B}}{\partial D_\star} &= \delta_{e_A, E} \sum_{q_B} f_B \mathbf{O}_{B\star} \left(f_\star \mathcal{D}_B + \frac{\partial f_\star}{\partial D_\star} \right) + \delta_{e_B, E} \sum_{q_A} f_A \mathbf{O}_{A\star} \left(f_\star \mathcal{D}_A + \frac{\partial f_\star}{\partial D_\star} \right) \end{aligned}$$

$$\begin{aligned}
\partial c_E^E &= \partial \left(\mathbf{G}_{EE} - \langle \psi^E | \left(\sum_{e_A, e_B}^{E-1} |\psi^{e_A}\rangle (\mathbf{G}^i)_{e_A e_B} \langle \psi^{e_B} | \right) | \psi^E \rangle \right)^{-\frac{1}{2}} = \\
&= -\frac{1}{2} \left(\mathbf{G}_{EE} - \sum_{e_A, e_B}^{E-1} \mathbf{G}_{Ee_A} (\mathbf{G}^i)_{e_A e_B} \mathbf{G}_{e_B E} \right)^{-\frac{3}{2}} \cdot \left(\partial \mathbf{G}_{EE} - \sum_{e_A, e_B}^{E-1} (\mathbf{G}^i)_{e_A e_B} (\partial(\mathbf{G}_{Ee_A}) \mathbf{G}_{e_B E} + \mathbf{G}_{Ee_A} \partial(\mathbf{G}_{e_B E})) \right) \\
\frac{\partial c_E^E}{\partial D_\star} &= (c_E^E)^3 \left((-1) \cdot \sum_{q_A} f_{q_A}^E \mathbf{O}_{q_A Q}^{E E} \left(f_\star \mathcal{D}_{q_A}^E + \frac{\partial f_\star}{\partial D_\star} \right) + \right. \\
&\quad \left. + \sum_{e_A}^{E-1} \sum_{e_B}^{E-1} (\mathbf{G}^i)_{e_A e_B} \mathbf{G}_{e_B E} \sum_{q_A} f_A \mathbf{O}_{A\star} \left(f_\star \mathcal{D}_A + \frac{\partial f_\star}{\partial D_\star} \right) \right) = \\
&\quad = (c_E^E)^3 \sum_{q_A, e_A} \mathcal{G}_{e_A} f_A \mathbf{O}_{A\star} \left(f_\star \mathcal{D}_A + \frac{\partial f_\star}{\partial D_\star} \right) \\
\partial c_e^E \{e \neq E\} &= \partial \left(- \sum_{e_A}^{E-1} (\mathbf{G}^i)_{ee_A} \mathbf{G}_{e_A E} c_E^E \right) = - \sum_{e_A}^{E-1} (\mathbf{G}^i)_{ee_A} (\mathbf{G}_{e_A E} \partial c_E^E + c_E^E \partial \mathbf{G}_{e_A E}) \\
\frac{\partial}{\partial D_\star} c_e^E \{e \neq E\} &= \left(- \mathcal{G}_e \frac{\partial c_E^E}{\partial D_\star} \right) - c_E^E \sum_{e_A}^{E-1} (\mathbf{G}^i)_{ee_A} \frac{\partial \mathbf{G}_{e_A E}}{\partial D_\star} = -c_E^E \sum_{e_A} \left(((c_E^E)^2 \mathcal{G}_e \mathcal{G}_{e_A} + \mathbf{G}^i_{ee_A}) \sum_{q_A} f_A \mathbf{O}_{A\star} \left(f_\star \mathcal{D}_A + \frac{\partial f_\star}{\partial D_\star} \right) \right)
\end{aligned}$$

because $\mathbf{G}^i_{E\bullet} = \mathbb{0}$, and using the definition of c_e^E ,

$$\frac{\partial c_e^E}{\partial D_\star} \{\forall e\} = -c_E^E \sum_{e_A} \left((c_e^E c_{e_A}^E + \mathbf{G}^i_{ee_A}) \sum_{q_A} f_A \mathbf{O}_{A\star} \left(f_\star \mathcal{D}_A + \frac{\partial f_\star}{\partial D_\star} \right) \right)$$

$$\begin{aligned}
\partial\rho^{AB} &= \partial\left(D_A(D_B^\top D_A)^{-1}D_B^\top\right) = \\
&= \partial(D_A)(D_B^\top D_A)^{-1}D_B^\top + D_A(D_B^\top D_A)^{-1}\partial D_B^\top - D_A(D_B^\top D_A)^{-1}\left(\partial(D_B^\top)D_A + D_B^\top\partial(D_A)\right)(D_B^\top D_A)^{-1}D_B^\top \\
\partial\rho_{m_1 m_2}^{A B} &= \partial\left(\mathbf{J}_{(m_1)}^\top \rho^{AB} \mathbf{J}_{(m_2)}\right) = \\
= \text{tr}\left(\mathbf{J}_{(m_2, m_1)} \partial\rho^{AB}\right) &= \text{tr}\left((D_B^\top D_A)^{-1}D_B^\top \mathbf{J}_{(m_2, m_1)}(\mathbb{1} - \rho^{AB})\partial D_A + (D_A^\top D_B)^{-1}D_A^\top \mathbf{J}_{(m_1, m_2)}(\mathbb{1} - \rho^{BA})\partial D_B\right) \\
\frac{\partial\rho_{m_1 m_2}^{A B}}{\partial D_\star} &= \delta_{A, \star} \mathcal{D}_B \mathbf{J}_{(m_2, m_1)} (\mathbb{1}_M - \rho^{*B}) + \delta_{B, \star} \mathcal{D}_A \mathbf{J}_{(m_1, m_2)} (\mathbb{1}_M - \rho^{*A})
\end{aligned}$$

$$\begin{aligned}
\partial\mathbf{H}_{AB} &= \partial\mathbf{O}_{AB} \sum_{\substack{m_1, m_2, \\ m_3, m_4}} \bar{H}_{m_1 m_2 m_3 m_4} \rho_{m_1 m_2}^{A B} \rho_{m_3 m_4}^{A B} = \\
= \mathbf{H}_{AB}(\mathcal{D}_B \partial D_A + \mathcal{D}_A \partial D_B) &+ \sum_{\substack{m_1, m_2, \\ m_3, m_4}} \underbrace{(\bar{H}_{m_1 m_2 m_3 m_4} + \bar{H}_{m_3 m_4 m_1 m_2})}_{\bar{\bar{H}}_{m_1 m_2 m_3 m_4}} \rho_{m_1 m_2}^{A B} \partial\rho_{m_3 m_4}^{A B}
\end{aligned}$$

$$\begin{aligned} \frac{\partial \mathbf{H}_{AB}}{\partial D_\star} &= \mathbf{H}_{AB}(\delta_{B,\star} \mathcal{D}_A + \delta_{A,\star} \mathcal{D}_B) + \delta_{B,\star} \left(\mathbf{O}_{A\star} \mathcal{D}_A \sum_{m_3, m_4} \rho_{m_3 m_4}^{A\star} \underbrace{\left(\sum_{m_1, m_2} \bar{\bar{H}}_{m_1 m_2 m_3 m_4} \mathbf{J}_{(m_1, m_2)} \right)}_{\bar{\bar{H}}_{\bullet\bullet m_3 m_4}} \right) (\mathbb{1}_M - \rho^{\star A}) + \\ &+ \delta_{A,\star} \left(\mathbf{O}_{B\star} \mathcal{D}_B \sum_{m_3, m_4} \rho_{m_3 m_4}^{\star B} \underbrace{\left(\sum_{m_1, m_2} \bar{\bar{H}}_{m_1 m_2 m_3 m_4} \mathbf{J}_{(m_2, m_1)} \right)}_{(\bar{\bar{H}}_{\bullet\bullet m_3 m_4})^\top} \right) (\mathbb{1}_M - \rho^{\star B}) \end{aligned}$$

$$\sum_{\substack{q_A, q_B, \\ e_A, e_B}} f_A f_B c_{e_A}^E c_{e_B}^E \frac{\partial}{\partial D_\star} \mathbf{H}_{AB} = f_\star c_E^E \sum_{q_A, e_A} f_A c_{e_A}^E \mathcal{D}_A \left(2\mathbf{H}_{A\star} \mathbb{1}_M + \mathbf{O}_{A\star} \left(\sum_{m_1, m_2} \rho_{m_1 m_2}^{A\star} \underbrace{\left(\bar{\bar{H}}_{\bullet\bullet m_1 m_2} + \bar{\bar{H}}_{\bullet\bullet m_2 m_1} \right)}_{\bar{\bar{H}}_{\bullet\bullet m_1 m_2}} \right) (\mathbb{1}_M - \rho^{\star A}) \right)$$

Finally

$$\begin{aligned}
\frac{\partial \mathcal{E}}{\partial D_\star} &= \sum_{q_A, e_A} f_A c_{e_A}^E c_E^E (\mathbf{H}_{A\star} + \mathbf{H}_{\star A}) \frac{\partial f_\star}{\partial D_\star} + \sum_{\substack{q_A, q_B, \\ e_A, e_B}} f_A f_B c_{e_A}^E (\mathbf{H}_{AB} + \mathbf{H}_{BA}) \frac{\partial c_{e_B}^E}{\partial D_\star} + \sum_{\substack{e_A, e_B, \\ q_A, q_B}} f_A f_B c_{e_A}^E c_{e_B}^E \frac{\partial}{\partial D_\star} \mathbf{H}_{AB} = \\
&= \sum_{q_A, e_A} f_A c_{e_A}^E c_E^E (\mathbf{H}_{A\star} + \mathbf{H}_{\star A}) \frac{\partial f_\star}{\partial D_\star} - \sum_{\substack{q_A, q_B, \\ q_C, e_A, \\ e_B, e_C}} f_A f_B c_{e_A}^E (\mathbf{H}_{AB} + \mathbf{H}_{BA}) c_E^E (c_{e_B}^E c_{e_C}^E + \mathbf{G}^i_{e_B e_C}) f_C \mathbf{O}_{C\star} \left(f_\star \mathcal{D}_C + \frac{\partial f_\star}{\partial D_\star} \right) + \\
&\quad + \sum_{\substack{e_A, e_B, \\ q_A, q_B}} f_A f_B c_{e_A}^E c_{e_B}^E \frac{\partial}{\partial D_\star} \mathbf{H}_{AB} = \\
&= \left(\sum_{q_A, e_A} 2 f_A c_{e_A}^E c_E^E \left(\mathbf{H}_{A\star} - \sum_{\substack{q_B, q_C, \\ e_B, e_C}} \mathbf{H}_{AB} f_B f_C \mathbf{O}_{C\star} (c_{e_B}^E c_{e_C}^E + \mathbf{G}^i_{e_B e_C}) \right) \right) \frac{\partial f_\star}{\partial D_\star} - \\
&\quad - \sum_{\substack{q_A, q_B, \\ q_C, e_A, \\ e_B, e_C}} 2 f_A f_B f_C f_\star c_{e_A}^E c_E^E \mathbf{H}_{AB} \mathbf{O}_{C\star} (c_{e_B}^E c_{e_C}^E + \mathbf{G}^i_{e_B e_C}) \mathcal{D}_C + \\
&\quad + f_\star c_E^E \sum_{q_A, e_A} f_A c_{e_A}^E \mathcal{D}_A \left(2 \mathbf{H}_{A\star} \mathbb{1}_M + \mathbf{O}_{A\star} \left(\sum_{m_1, m_2} \rho_{m_1 m_2}^{A\star} \bar{\bar{H}}_{\bullet\bullet m_1 m_2} \right) (\mathbb{1}_M - \rho^{\star A}) \right) = \\
&= 2 c_E^E \left(\sum_{q_A, e_A} c_{e_A}^E f_A \left(\mathbf{H}_{A\star} - \varepsilon \mathbf{O}_{A\star} - \sum_{q_B, e_B} f_B \mathbf{H}_{AB} \sum_{q_C, e_C} \mathbf{G}^i_{e_B e_C} f_C \mathbf{O}_{C\star} \right) \right) \frac{\partial f_\star}{\partial D_\star} + \\
&\quad + 2 c_E^E f_\star \left(\sum_{q_A, e_A} c_{e_A}^E f_A (\mathbf{H}_{A\star} - \varepsilon \mathbf{O}_{A\star}) \mathcal{D}_A \right) - 2 c_E^E f_\star \sum_{\substack{q_A, q_B, \\ e_A, e_B}} c_{e_A}^E f_A f_B \mathbf{H}_{AB} \sum_{q_C, e_C} \mathbf{G}^i_{e_B e_C} f_C \mathbf{O}_{C\star} \mathcal{D}_C + \\
&\quad + c_E^E f_\star \sum_{q_A, e_A} c_{e_A}^E f_A \mathbf{O}_{A\star} \mathcal{D}_A \left(\sum_{m_1, m_2} \rho_{m_1 m_2}^{A\star} \bar{\bar{H}}_{\bullet\bullet m_1 m_2} \right) (\mathbb{1}_M - \rho^{\star A}) =
\end{aligned}$$

$$= 2c_E^E \left(\sum_{q_A, e_A} W_A \right) \frac{\partial f_\star}{\partial D_\star} + c_E^E f_\star \sum_{q_A, e_A} \mathcal{D}_A \left(2W_A \mathbb{1}_M + c_{e_A}^E f_A \mathbf{O}_{A^\star} \left(\sum_{m_1, m_2} \rho_{m_1 m_2}^{A^\star} \bar{\bar{H}}_{\bullet \bullet m_1 m_2} \right) (\mathbb{1}_M - \rho^{\star A}) \right)$$

with

$$W_A = c_{e_A}^E f_A \left(\mathbf{H}_{A^\star} - \varepsilon \mathbf{O}_{A^\star} \sum_{q_B, e_B} \mathbf{G}_{e_A e_B}^i f_B \sum_{q_C, e_C} c_{e_C}^E f_C \mathbf{H}_{CB} \right)$$
